Check for updates

Global Ecology and Biogeography

WILEY

Global Ecology and Biogeography | A Journal of Macroecology

METHOD OPEN ACCESS

Generating Spatialised and Seasonal Deep-Time Palaeoclimatic Information: Integration Into an Environmental-Dependent Diversification Model

Delphine Tardif[1,2] | Fabien L. Condamine[3] | Serafin J. R. Streiff[1] | Pierre Sepulchre[2] | Thomas L. P. Couvreur[1]

[1]IRD, DIADE, University of Montpellier, Montpellier, France | [2]Laboratoire des Sciences du Climat et de l'Environnement, LSCE/IPSL, CEA-CNRS-UVSQ, Université Paris-Saclay, Gif-sur-Yvette, France | [3]CNRS, Institut des Sciences de l'Evolution de Montpellier, Université de Montpellier, Montpellier, France

Correspondence: Delphine Tardif (delphine.tardif@hotmail.fr)

Received: 16 May 2024 | **Revised:** 3 February 2025 | **Accepted:** 15 February 2025

Handling Editor: Moriaki Yasuhara

Funding: T.L.P.C. received funding from the European Research Council (ERC) under the European Union's Horizon 2020 research and innovation programme (project GLOBAL grant agreement no. 865787). F.L.C. received funding from the European Research Council (ERC) under the European Union's Horizon 2020 research and innovation programme (project GAIA, agreement no. 851188).

Keywords: macroevolution | palaeoclimate | palaeoenvironment-dependent model | regional temperature | seasonal temperature | temporal interpolation

ABSTRACT

Aim: Testing the impact of climate on diversification is a major goal of evolutionary biology. Birth-death models like palaeoenvironment-dependent diversification (PDD) models, for example, allow exploring the potential correlations between diversification dynamics and past environmental changes, such as temperature, among other abiotic variables. So far, such studies have been limited to proxy-derived global temperature trends, because these are the only temperature records that are easily accessible and almost continuous over multimillion-year periods.

Innovation: In this study, we propose a methodology to generate spatialised and/or seasonal palaeotemperature time series. To do so, we take advantage of temperature variables simulated by climate models for several 'snapshots' of the last 100 million years. Based on the hypothesis that a long-term global temperature drift is imprinted, to some degree, on all regional and seasonal temperature records, we use the global proxy-derived temperature record as the mean of interpolation between discrete climate simulations. We then evaluate the possibility of constraining the PDD models, as implemented in RPANDA, with these hybrid temperature time series. We assess if these regional and seasonal temperature trends may be more relevant to the evolutionary history of a given clade than the global temperature record used so far.

Main Conclusions: Our results show that PDD models using seasonal and/or regional hybrid temperature time series tend to receive high statistical support. This offers promising perspectives for refining our understanding of the impact of regional and seasonal temperature evolution on diversification dynamics, and calls for continuing development of deep-time palaeoclimate modelling and interdisciplinary studies.

This is an open access article under the terms of the Creative Commons Attribution-NonCommercial-NoDerivs License, which permits use and distribution in any medium, provided the original work is properly cited, the use is non-commercial and no modifications or adaptations are made.

© 2025 The Author(s). *Global Ecology and Biogeography* published by John Wiley & Sons Ltd.

1 | Introduction

Understanding the relative impact of biotic versus abiotic factors on species diversity is a key challenge in macroevolution (Ezard et al. 2016). It has long been addressed by assessing correlations between fossils or dated phylogenetic trees with the evolution of environmental parameters, such as proxy-derived global temperature, or uplift rates of mountain ranges (Hoorn et al. 2010; Jaramillo et al. 2006; Favre et al. 2015; Delsuc et al. 2004). In the past decades, steps forward have been made in the comprehension and formal quantification of these links. Palaeoenvironment-dependent diversification (PDD) models, such as implemented in RPANDA (Condamine et al. 2013), using time-calibrated molecular phylogenetic trees, are able to detect correlates between extinction and speciation rates, and an environmental parameter that varies through time. To this end, benthic marine sediments (Zachos et al. 2001; Westerhold et al. 2020) are extensively used as a proxy for deep-time palaeoclimate change. Indeed, their temporal resolution (typically of several thousands of years) is suitable for simple interpolations and the production of an almost time-continuous record needed in PDD models. Specifically, PDD models have been used with the Cenozoic and Cretaceous marine records of $\delta^{18}O$ oxygen isotopes (Westerhold et al. 2020; Veizer and Prokoph 2015) and the corresponding global temperature fluctuations (Condamine et al. 2013; Boschman and Condamine 2022). Other environmental variables tested in PDD models also include, but are not limited to, reconstructions of atmospheric CO_2 concentration (Lewitus et al. 2018), sea-level fluctuations (Condamine et al. 2015), $\delta^{13}C$ (Lewitus and Morlon 2018) and topographic changes (Boschman and Condamine 2022; Dagallier et al. 2024; Lagomarsino et al. 2016).

The use of a variable describing the evolution of global climate in a diversification model nevertheless raises the question of its relevance in explaining speciation and/or extinction dynamics of a group that has diversified regionally rather than globally. One can assume that using a global climate indicator is likely to be relevant if applied to a widespread clade, but may be less appropriate if applied to a continental endemic clade or a regionally restricted clade. Indeed, atmospheric (e.g., monsoon regions) and ocean (e.g., upwelling regions) dynamics, latitude (e.g., polar amplification), land-sea distribution or mountain uplift create climatic heterogeneity in space and time. We could also expect that seasonality, rather than annual averages, could be more relevant for diversification dynamics of certain groups: for example, winter temperature was suggested to be a highly constraining factor for ectotherm animals (Chiarenza et al. 2023) or tropical plant dispersal out of low latitudes (Donoghue 2008).

With this in mind, recent studies have attempted to integrate regional environmental data by developing different strategies. The first choice is usually to use regional field data when such records are available at suitable temporal resolution. For example, Weppe et al. (2023) evaluated the impact of regional abiotic parameters on European artiodactyl turnover at the Eocene–Oligocene Transition, using mean annual and seasonal European palaeoclimatic records from Mosbrugger et al. (2005). However, generating regional environmental time series over multimillion-year periods and with an appropriate resolution remains a challenge, as data are temporally sparse and spatially scattered. To circumvent this issue, methodologies combining field data and numerical tools are interesting. In order to study the diversification of North American freshwater gastropods over the last 200 Ma, Neubauer et al. (2022) extracted a subset of North American mean annual temperatures, with one value every 5 Ma, from a global palaeoclimate simulations data set (the PALEOMAP project, see Valdes et al. (2021), Scotese and Wright (2018)). However, the need for records with a finer time resolution (less than 1 Myr) quickly leads to significant computational limitations with complex Earth System Models, making it impossible to produce multimillion-year transient palaeoclimate simulations. Such limitations may be overcome by using a set of palaeoclimate simulations, which provide physically coherent, spatialised climatic 'snapshots', and to use an interpolation method to produce continuous abiotic time series between these 'snapshots'. To this end, previous studies have efficiently developed statistical emulators (Lord et al. 2017; Van Breedam et al. 2021). Providing a few simulations describing the Earth's climatic conditions under a variety of scenarios (e.g., in extreme orbital configurations with corresponding ice-sheet configurations), the emulator is able to predict the climatic variables for any combination of the forcing parameters within the domain of the end-member simulations. Such methods so far have been used for periods spanning less than 10 million years (My).

Here, we set forth an alternative hybrid approach, that leans on the wide range of temperature output variables that Earth System Models calculate, while still benefiting from the high temporal resolution information retrieved from sedimentary archives. The following framework allows generating custom-designed regional palaeoclimate data across the last 100 My, and potentially longer periods. We take advantage of temperature outputs from a recently published palaeoclimate simulation data set (Li et al. 2022) generated with the Community Earth System Model (CESM). Each simulation is a discrete climatic 'snapshot', providing monthly temperatures at any point of the globe every 10 My. We then introduce a novel interpolation methodology, using a kriging interpolation (see Section 2.2.3), allowing to use the global temperature trend provided by proxy records to fill the gaps between the simulated climate snapshots. These hybrid temperature time series are then fed into the RPANDA PDD model to evaluate their potential for explaining diversification dynamics. As such, we (i) compared this new approach with the traditional use of the global $\delta^{18}O$ temperature proxy-derived curve, and (ii) explored the importance of regional and seasonal climate changes by applying them to a set of clades with different spatial distributions and biogeographic histories spanning the last 100 My.

2 | Materials and Methods

2.1 | Choice of Biological Groups and Phylogenetic Data

We selected a number of biological groups (Table 1) with near-complete, robust dated phylogenetic trees available at the time of this study. The origin of each group is estimated within the past 100 My before present (hereafter Ma), which allows the use of the composite proxy-derived global temperature time series introduced in previous studies (Boschman and Condamine 2022;

TABLE 1 | Tested phylogenies, sampling fraction and missing species, age of clade and distribution.

Clade name	Sampling fraction (missing species)	Clade age (Ma)	Distribution	Reference
Global				
Cetacea	87/89 (2)	35	Global oceanic	Steeman et al. (2009)
Testudinoidea	160/177 (17)	91	Global terrestrial	Thomson et al. (2021)
Regional (terrestrial)				
Monodorae	88/90 (2)	25	Afrotropics	Dagallier et al. (2024)
Pinus	116/122 (6)	90	Holarctic, mountainous	Leslie et al. (2018)
Parnassiinae	85/90 (5)	39	Holarctic, mountainous	Condamine et al. (2018)
Arinae	167/150 (0)	24	Neotropics	Smith et al. (2023)
Thamnophilidae	231/236 (5)	19	Neotropics	Harvey et al. (2020)

Condamine et al. 2013). We chose clades spanning a range of different spatial (global and regional) and environmental settings (tropical and temperate, mountainous and lowland). This nonexhaustive selection of clades allowed us to test different types of temperature time series, from the more global to the more regional and/or seasonal, based on the general ecology of each group. Each clade is briefly presented, together with the hypothesis we wish to test related to their diversification dependence on temperature.

2.1.1 | Cetacea

Cetacea are an infraorder of aquatic mammals with approximately 89 living species separated into two parvorders: Odontoceti, or toothed whales (containing porpoises, dolphins, other predatory whales like the beluga, the sperm whale and the beaked whales) and the filter-feeding Mysticeti, or baleen whales (which includes species like the blue whale, the humpback whale and the bowhead whale). Having a cosmopolitan distribution, they can be found in some rivers and all of Earth's oceans, and many species inhabit vast ranges where they migrate with the changing of the seasons. We retrieved the species-level time-calibrated phylogenetic tree of Cetacea, with an origin dated around 35 Ma and that includes most species, that is, 87 of the 89 species (Steeman et al. 2009), which has been used in several diversification studies to test birth-death models (Morlon et al. 2011; Condamine et al. 2013). With the Cetacean phylogeny, we compared the support received by environment-dependent models using the traditional proxy-derived global temperature time series and those using sea surface temperature time series reconstructed with our hybrid method.

2.1.2 | Testudinoidea

Within the order Testudines (turtles), Testudinoidea is a superfamily including the pond turtles (family Emydidae), Asian turtles (family Geoemydidae), the monotypic big-headed turtle (family Platysternidae) and the tortoises (family Testudinidae), for a total of 177 extant species (Thomson et al. 2021). Their origin is estimated around 91 Ma; they are well spread over the globe, with a strong affinity for low-elevation and coastal environments. Although currently distributed preferentially in tropical and subtropical environments, the fossil record indicates a more widespread distribution, up to the polar regions during warmer climates, especially in the Cretaceous (Chiarenza et al. 2023). Palaeoniche modelling studies have highlighted that temperature (both annual and seasonal) is a critical abiotic driver of turtle species distribution (Chiarenza et al. 2023). Therefore, we explored the impact of mean annual and coldest month temperature evolution on Testudinoidea diversification. Given their cosmopolitan distribution, all available continental temperature time series have been tested (global and regional).

2.1.3 | Pinus

Pinus is a genus of conifers, comprising the sections *Pinus* (subsections *Pinus* and *Pinaster*), mostly present in the Palearctic and the section *Trifoliae* (subsections *Australes*, *Ponderosae*, *Contortae*, *Attenuatae*, *Sabinianae*), mostly present in the Nearctic region (Jin et al. 2021). We retrieved the phylogenetic tree from Leslie et al. (2018), for a total of 122 species, with an origin dated in the Late Cretaceous (around 90 Ma). The extant species richness of *Pinus* is spread across the Holarctic region, occupying arid to subtropical environments, with an affinity for mountainous settings (Nobis et al. 2012). The relationship between predictor variables and current species richness has highlighted a positive correlation of *Pinus* species richness with topography and temperature (Jin et al. 2021). Therefore, in addition to global temperature-dependent models, we tested here the potential correlations of diversification with regional temperature time series of the Eurasian and North American continents, respectively. We also explored possible correlation to seasonal trends (coldest month evolution) and to plains or mountainous environments temperature evolution.

2.1.4 | Parnassiinae

Within swallowtail butterflies, the subfamily Parnassiinae (Apollo butterflies) comprises eight genera with around 90 currently recognised species, grouped into three tribes: Luehdorfiini,

Sericinini and Parnassiini (Condamine et al. 2013). Apollo butterflies occur from the western Palearctic to the western Nearctic. Most of the species' richness is concentrated in the Palearctic, where there are two nonmonophyletic lowland-flying communities separated by the Himalayas and the Tibetan Plateau: An Eastern Palearctic group formed by *Luehdorfia* (Luehdorfiini) and *Bhutanitis* and *Sericinus* (Sericinini), and a Western Palearctic community including *Archon* (Luehdorfiini), *Allancastria* and *Zerynthia* (Sericinini), and *Hypermnestra* (Parnassiini). The most speciose genus, *Parnassius*, is mainly distributed in mountainous regions throughout the Holarctic, with its highest diversity in the Himalaya and Tibetan Plateau. Apollo butterflies provide a model for understanding the role of past environmental change in diversification because they are adapted to cold climates and occur in high mountains of the Northern Hemisphere. A previous study has found an effect of temperature and Himalayan orogeny on their diversification (Condamine et al. 2018). Phylogeographic studies have revealed an effect of Pleistocene glaciations on population-level dynamics (Dapporto 2009; Todisco et al. 2010, 2012; Zinetti et al. 2013). Time-calibrated phylogenies support an early Cenozoic origin of the subfamily (Condamine et al. 2018; Allio et al. 2021), which means that the lineage has experienced the dramatic cooling and warming events of the last 50 My, including a drop in global temperatures during the Eocene–Oligocene climate transition that led to the demise of Boreotropical Holarctic vegetation (Condamine et al. 2018). Therefore, we investigated the impact of mean annual and coldest month temperature evolution on Apollo diversification. Given their distribution, we tested correlations of diversification with temperature time series of the Eurasian and North American continents, and with temperature evolution in plains or mountainous environments.

2.1.5 | Monodoreae

The African subtribe Monodoreae belongs to the large pantropical plant family Annonaceae (Chatrou et al. 2012). This clade contains 90 currently recognised species of mainly trees in 11 genera (Dagallier et al. 2023). Most species are restricted to the lowland rain forests of west, central and east Africa, with a few species also occurring in Madagascar (five species of the genus *Isolona*; Couvreur 2009). A recent near-complete species-level phylogenomic study estimated the origin of Monodoreae at around 25 Ma (Dagallier et al. 2024), that is at the start of the Miocene. For this group, we tested the impact of mean annual and coldest month temperature in plains in Africa (Table 2).

2.1.6 | Neotropical Birds: Arinae and Thamnophilidae

We analysed two clades of Neotropical birds. One is within the order of parrots, Arinae (Neotropical parrots or New World parrots), which is a subfamily of the Psittacidae, comprising about 160 extant species in 32 genera found throughout South and Central America and the Caribbean islands. The origin of the subfamily is dated around 24 Ma and is further divided into four tribes (Smith et al. 2023). The group is mostly distributed in Amazonian forests, in particular along river systems. The other study group is the Thamnophilidae (antbirds), a family of Neotropical birds comprising 236 extant species dated around 19 Ma and belonging to the infraorder Furnariides (Harvey et al. 2020). They are found across subtropical and tropical Central and South America. Most species live in forests and feed in the understory and midstory of the forest. For both clades, there is no strong evidence that diversification would be influenced by climate or elevation (Harvey et al. 2020; Smith et al. 2023). In this case, we tested the impact of mean annual and coldest month temperature in South America (Table 2) and with temperature in plains or mountainous regions.

2.2 | Choice of Climate Variables

Climate change at the geological timescale involves variations in numerous physical variables (e.g., temperature, rainfall, wind velocity and ocean surface salinity) that can impact environments and diversity. Here we have restricted our study to temperature, which has the best-documented record for the Phanerozoic and is the most robust in palaeoclimate numerical simulations.

2.2.1 | Global Proxy-Derived Temperature Time Series

The Global Air Temperature time series (GATdat, Figure 1) is derived from palaeoceanographic isotopic records. It is obtained by combining the $\delta^{18}O$ Cenozoic data set from Westerhold et al. (2020) with the Cretaceous data set from Veizer and Prokoph (2015), as introduced in Boschman and Condamine (2022). $\delta^{18}O$ values measured on benthic foraminifera are converted to deep-sea temperature, then to global air temperature using the equations described in Hansen et al. (2013). Given that the typical time resolution of the deep-sea record is of thousands to ten of thousands of years, a continuous estimate of global air temperature through time has been calculated by applying a smoothing spline (*degrees of freedom*: 80) on bulk data, to provide a reliable estimate of global temperature trend through time. Such a global temperature data set has been classically used in phylogenetic diversification studies, even for regionally distributed clades (Condamine et al. 2013; Davis et al. 2016; Condamine et al. 2018, 2019; Dagallier et al. 2024).

2.2.2 | Temperature Variables Extracted From Palaeoclimate Simulations

We utilised a high-resolution (0.9° latitude × 1.25° longitude) data set of palaeoclimate simulations recently generated using the Community Earth System Model (CESM) version 1.2.2 (Li et al. 2022). The data set covers the entire Phanerozoic (last 540 My) and includes one simulation every 10 My. We extracted a subset of 11 simulations covering the last 100 My, each simulation providing a spatially-gridded 'snapshot' of steady-state climate variables for a given time period (at 100, 90, 80 Ma, etc.). Variables are in the form of an averaged climatology, that is, 12 monthly outputs, spatialised over the globe (see Supporting Information for detailed step-by-step tutorial). The globally and yearly averaged air temperature over land and sea (GAT, for Global Air Temperature) is thus comparable to the proxy-derived GATdat variable introduced earlier, and has been used as a first test for our new approach (Figure 1a).

TABLE 2 | Summary of the 86 models fitted in RPANDA.

Type of model	Description	Equation	Parameters	Acronym
14 models tested on all phylogenies				
Constant-rate	Constant speciation and no extinction	$\lambda(t) = \lambda_0; \mu(t) = 0$	1	**B**
	Constant speciation and extinction	$\lambda(t) = \lambda_0; \mu(t) = \mu_0$	2	**B_D**
Time-dependent	Speciation variable and no extinction	$\lambda(t) = \lambda_0 e^{\alpha t}; \mu(t) = 0$	2	**B***Time*
	Speciation variable and constant extinction	$\lambda(t) = \lambda_0 e^{\alpha t}; \mu(t) = \mu_0$	3	**B***Time*_**D**
	Constant speciation and extinction variable	$\lambda(t) = \lambda_0; \mu(t) = \mu_0 e^{\beta t}$	3	**B_D***Time*
	Both speciation and extinction variable	$\lambda(t) = \lambda_0 e^{\alpha t}; \mu(t) = \mu_0 e^{\beta t}$	4	**B***Time*_**D***Time*
Global air temperature-dependent (GATdat, GAT)	Speciation variable and no extinction	$\lambda(t) = \lambda_0 e^{\alpha T(t)}; \mu(t) = 0$	2	**B***GATdat*; **B***GAT*
	Speciation variable and constant extinction	$\lambda(t) = \lambda_0 e^{\alpha T(t)}; \mu(t) = \mu_0$	3	**B***GATdat*_**D**; **B***GAT*_**D**
	Constant speciation and extinction variable	$\lambda(t) = \lambda_0; \mu(t) = \mu_0 e^{\beta T(t)}$	3	**B_D***GATdat*; **B_D***GAT*
	Both speciation and extinction variable	$\lambda(t) = \lambda_0 e^{\alpha T(t)}; \mu(t) = \mu_0 e^{\beta T(t)}$	4	**B***GATdat*_**D***GATdat*; **B***GAT*_**D***GAT*
Four temperature-dependent models tested on marine phylogeny *Cetacea*				
SST	Speciation variable and no extinction	$\lambda(t) = \lambda_0 e^{\alpha T(t)}; \mu(t) = 0$	2	**B***SST*
	Speciation variable and constant extinction	$\lambda(t) = \lambda_0 e^{\alpha T(t)}; \mu(t) = \mu_0$	3	**B***SST*_**D**
	Constant speciation and extinction variable	$\lambda(t) = \lambda_0; \mu(t) = \mu_0 e^{\beta T(t)}$	3	**B_D***SST*
	Both speciation and extinction variable	$\lambda(t) = \lambda_0 e^{\alpha T(t)}; \mu(t) = \mu_0 e^{\beta T(t)}$	4	**B***SST*_**D***SST*
Eight temperature-dependent models tested on continental phylogenies: *Testudinoidea, Pinus, Parnassiinae, Arinae, Monodorae*				

(Continues)

TABLE 2 | (Continued)

Type of model	Description	Equation	Parameters	Acronym
MAT, CMT	Speciation variable and no extinction	$\lambda(t) = \lambda_0 e^{\alpha T(t)}; \mu(t) = 0$	2	**B***MAT*; **B***CMT*
	Speciation variable and constant extinction	$\lambda(t) = \lambda_0 e^{\alpha T(t)}; \mu(t) = \mu_0$	3	**B***MAT*_**D**; **B***CMT*_**D**
	Constant speciation and extinction variable	$\lambda(t) = \lambda_0; \mu(t) = \mu_0 e^{\beta T(t)}$	3	**B_D***MAT*; **B_D***CMT*
	Both speciation and extinction variable	$\lambda(t) = \lambda_0 e^{\alpha T(t)}; \mu(t) = \mu_0 e^{\beta T(t)}$	4	**B***MAT*_**D***MAT*; **B***CMT*_**D***CMT*
32 temperature-dependent models tested on holarctics phylogenies *Pinus, Parnassiinae* and on global phylogeny *Testudinoidea*				

(Continues)

TABLE 2 | (Continued)

Type of model	Description	Equation	Parameters	Acronym
MAT-EURA-P, MAT-EURA-M, CMT-EURA-P, CMT-EURA-M, MAT-NAM-P, MAT-NAM-M, CMT-NAM-P, CMT-NAM-M	Speciation variable and no extinction	$\lambda(t) = \lambda_0 e^{\alpha T(t)}; \mu(t) = 0$	2	**B***MAT-EURA-P*; **B***MAT-EURA-M*
				B*CMT-EURA-P*; **B***CMT-EURA-M*
				B*MAT-NAM-P*; **B***MAT-NAM-M*
				B*CMT-NAM-P*; **B***CMT-NAM-M*
	Speciation variable and constant extinction	$\lambda(t) = \lambda_0 e^{\alpha T(t)}; \mu(t) = \mu_0$	3	**B***MAT-EURA-P*_**D**; **B***MAT-EURA-M*_**D**
				B*CMT-EURA-P*_**D**; **B***CMT-EURA-M*_**D**
				B*MAT-NAM-P*_**D**; **B***MAT-NAM-M*_**D**
				B*CMT-NAM-P*_**D**; **B***CMT-NAM-M*_**D**
	Constant speciation and extinction variable	$\lambda(t) = \lambda_0; \mu(t) = \mu_0 e^{\beta T(t)}$	3	**B_D***MAT-EURA-P*; **B_D***MAT-EURA-M*
				B_D*CMT-EURA-P*; **B_D***CMT-EURA-M*
				B_D*MAT-NAM-P*; **B_D***MAT-NAM-M*
				B_D*CMT-NAM-P*; **B_D***CMT-NAM-M*
	Both speciation and extinction variable	$\lambda(t) = \lambda_0 e^{\alpha T(t)}; \mu(t) = \mu_0 e^{\beta T(t)}$	4	**B***MAT-EURA-P*_**D***MAT-EURA-P*
				B*MAT-EURA-M*_**D***MAT-EURA-M*
				B*CMT-EURA-P*_**D***CMT-EURA-P*
				B*CMT-EURA-M*_**D***CMT-EURA-M*
				B*MAT-NAM-P*_**D***MAT-NAM-P*
				B*MAT-NAM-M*_**D***MAT-NAM-M*
				B*CMT-NAM-P*_**D***CMT-NAM-P*
				B*CMT-NAM-M*_**D***CMT-NAM-M*
16 temperature-dependent models tested on Neotropical phylogeny *Arinae* and on global phylogeny *Testudinoidea*				

(Continues)

TABLE 2 | (Continued)

Type of model	Description	Equation	Parameters	Acronym
MAT-SAM-P, MAT-SAM-M, CMT-SAM-P, CMT-SAM-M	Speciation variable and no extinction	$\lambda(t) = \lambda_0 e^{\alpha T(t)}; \mu(t) = 0$	2	**B***MAT-SAM-P*; **B***MAT-SAM-M* **B***CMT-SAM-P*; **B***CMT-SAM-M*
	Speciation variable and constant extinction	$\lambda(t) = \lambda_0 e^{\alpha T(t)}; \mu(t) = \mu_0$	3	**B***MAT-SAM-P*_**D**; **B***MAT-SAM-M*_**D** **B***CMT-SAM-P*_**D**; **B***CMT-SAM-M*_**D**
	Constant speciation and extinction variable	$\lambda(t) = \lambda_0; \mu(t) = \mu_0 e^{\beta T(t)}$	3	**B_D***MAT-SAM-P*; **B_D***MAT-SAM-M* **B_D***CMT-SAM-P*; **B_D***CMT-SAM-M*
	Both speciation and extinction variable	$\lambda(t) = \lambda_0 e^{\alpha T(t)}; \mu(t) = \mu_0 e^{\beta T(t)}$	4	**B***MAT-SAM-P*_**D***MAT-SAM-P* **B***MAT-SAM-M*_**D***MAT-SAM-M* **B***CMT-SAM-P*_**D***CMT-SAM-P* **B***CMT-SAM-M*_**D***CMT-SAM-M*
Eight temperature-dependent models tested on African phylogeny *Monodorae* and on global phylogeny *Testudinoidea*				
MAT-AFR-P, CMT-AFR-P	Speciation variable and no extinction	$\lambda(t) = \lambda_0 e^{\alpha T(t)}; \mu(t) = 0$	2	**B***MAT-AFR-P*; **B***CMT-AFR-P*
	Speciation variable and constant extinction	$\lambda(t) = \lambda_0 e^{\alpha T(t)}; \mu(t) = \mu_0$	3	**B***MAT-AFR-P*_**D**; **B***CMT-AFR-P*_**D**
	Constant speciation and extinction variable	$\lambda(t) = \lambda_0; \mu(t) = \mu_0 e^{\beta T(t)}$	3	**B_D***MAT-AFR-P*; **B_D***CMT-AFR-P*
	Both speciation and extinction variable	$\lambda(t) = \lambda_0 e^{\alpha T(t)}; \mu(t) = \mu_0 e^{\beta T(t)}$	4	**B***MAT-AFR-P*_**D***MAT-AFR-P* **B***CMT-AFR-P*_**D***CMT-AFR-P*

Note: For the temperature-dependent models, the four models in the description were fitted for each temperature variable (e.g., GAT, MAT, CMT) introduced in Figure 1.

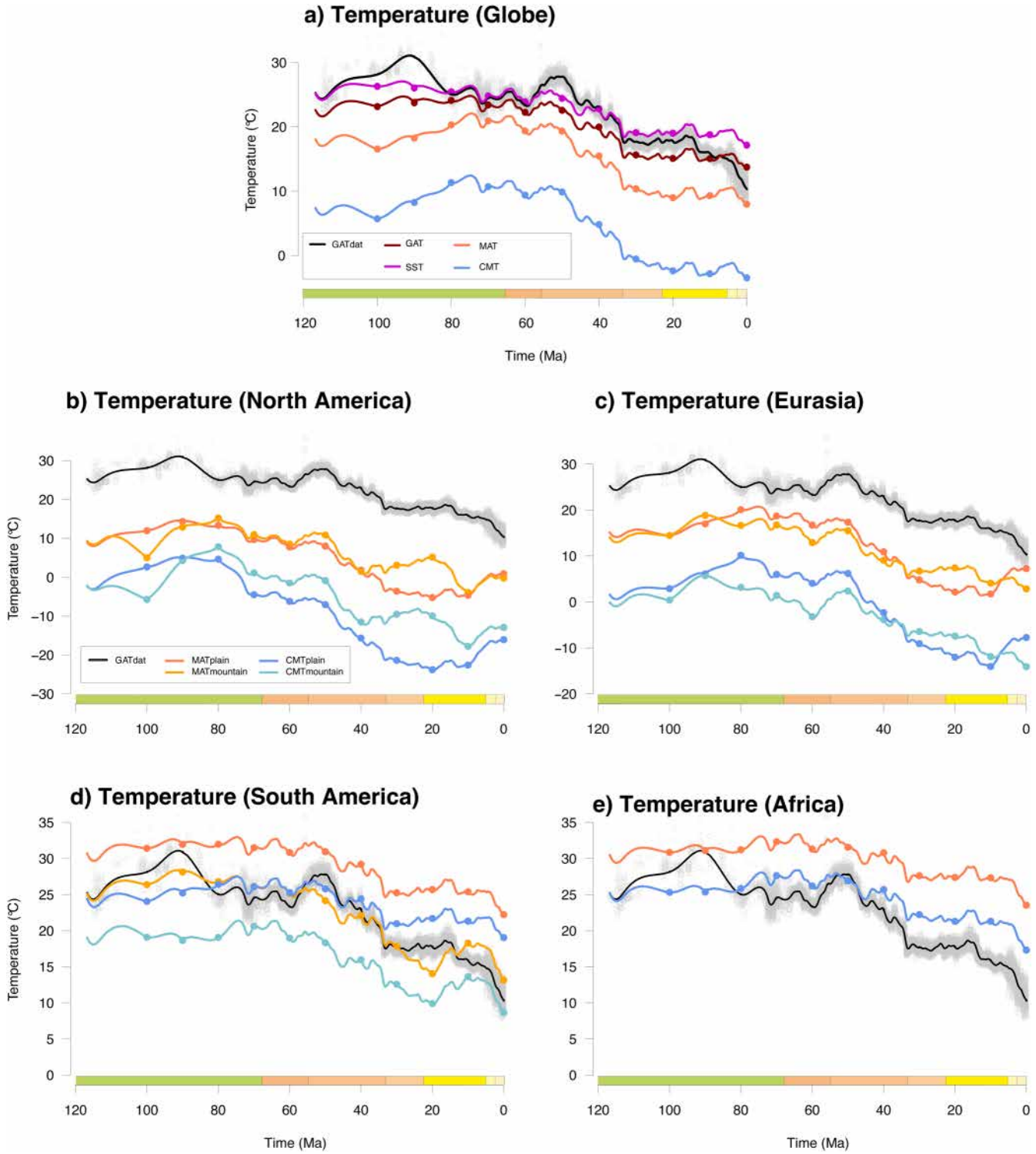

FIGURE 1 | Environmental variables used in the present study. (a) Global Annual Temperature, either derived from proxies (GATdat) or reconstructed with the hybrid methodology: (GAT), continental mean annual temperature (MAT) and winter temperature (CMT) and sea surface temperature (SST); (b-e) At a regional scale, MAT and CMT are distinguished either by considering only continental areas below 1000 m of altitude (MATplain, CMTplain) and above 1000 m (MATmountain, CMTmountain), for (c) North America, (d) Eurasia, (e) South America, (f) Africa. Coloured circles each 10 Ma in plots b to f represent the temperature obtained from palaeoclimate simulations, while the curves are obtained by applying a Kriging interpolation method, using the GATdat curve as trend (see Section 2.2.3). Note the change of scale on the temperature axis depending on each region.

We then extracted time series describing the mean annual evolution of air temperature over landmasses mean annual temperature (MAT) and above the sea surface (SST), averaged globally (Figure 1a). We acknowledge that a data set providing actual SST values (i.e., water surface temperature instead of air temperature above water) would likely produce slightly

different SST trends and that we are realising an approximation. Continental temperature time series of North America (suffix 'NAM'), Eurasia ('EURA'), South America ('SAM') and Africa ('AFR') were also extracted (Figure 1b–e). In addition, we distinguished between plain, or low-elevation lands (< 1000 m above sea level [asl], suffix 'P' in model names) from mountainous regions (> 1000 m asl, suffix 'M' in model names). We also extracted the Coldest Month Temperature averaged over all landmasses (CMT), as well as over previously mentioned continents, with the same elevation distinction. Note that for Africa, we only retained the low-elevation curves (*MAT-AFR-P* and *CMT-AFR-P*), due to inconsistencies regarding mountain uplift history in the palaeogeography that was used for the simulations (see Figures S2 and S3 with the South African Dome being fully uplifted at 30 and 10 Ma, but not at 20 Ma). Mapped regional and seasonal temperature outputs plotted for each palaeoclimate simulation are provided in Figures S1–S9.

2.2.3 | Time Interpolation of Simulated Palaeotemperatures

Since the PDD models require environmental variables defined continuously over time, the main challenge of our study was to interpolate between the discrete values simulated every 10 Ma (circles in Figure 1). Indeed, even though each simulation provides a fair description of the climate of the targeted period, it is missing important climate events occurring in between these time frames. For example, the Eocene–Oligocene Transition, dated at 33.9 Ma, and characterised by a sharp decrease in global temperatures and glacial inception, would not be visible. Therefore, we applied a one-dimensional Regression Kriging (Hengl et al. 2007), an interpolation method that uses the available proxy-derived global temperature trend (GATdat) as interpolation background for simulated temperatures. This approach assumes that temperature evolution over geological timescales imprints a global trend on any temperature signals, whether annual, seasonal, global, regional, marine or continental, despite the fact that these individual signals may show variations in the magnitude of the temperature shift.

The Kriging interpolation (see Hengl et al. (2007), for examples) is performed using the Gstat R package (Pebesma 2004). Kriging is a geostatistical method commonly used in geosciences to interpolate spatially and/or temporally autocorrelated variables based on a weighted average of available sampled points. The Regression Kriging (as well as other more complex methods such as Co-Kriging) is specifically adapted to interpolate a high-confidence, under-sampled target variable (here, the 11 discrete temperatures values extracted from our 11 palaeoclimate simulations subset) by using one or several well-sampled auxiliary variables (here, the proxy-derived global temperature trend) that are correlated to the target variable. This method allows for locally matching the discrete simulated values and follows the background trend provided by the proxy-derived curve for the interpolation (Figure 1). The Regression Kriging is done in several steps: (i) the covariance structure of the sampled points (temperature variables derived from palaeoclimate simulations, constituting here a set of 11 points, one each 10 Ma) is determined by fitting a variogram model to the experimental variogram, (ii) the residuals between simulated values and data-derived values are calculated, (iii) weights derived from this covariance structure are used to interpolate values for unsampled points (see expanded methodology in Figure S3). The degree of temporal refinement given by this final hybrid curve is thus highly dependent on the GATdat curve used as interpolation background material. While all curves presented here were obtained using a GATdat curve obtained with 80° of freedom, a much smoother GATdat background curve was also tested for benchmarking purposes (with 20° of freedom). As it received consistently lesser statistical support than the temperature curves obtained with the refined GATdat when used in RPANDA, results are not shown here.

2.3 | Estimating the Environment-Dependent Diversification With RPANDA

2.3.1 | The RPANDA Approach

Explicit environment-dependent diversification models have been developed in the last decade (Condamine et al. 2013; Davis et al. 2016). The approach used in this study, developed by Condamine et al. (2013, 2019), builds on time-dependent diversification models (Nee et al. 1994; Morlon et al. 2011) but allows speciation and extinction rates to depend on an external time-varying variable. This methodology is implemented in the R package RPANDA (Morlon et al. 2016). Under a constant birth-death process, clades are assumed to evolve with both speciation and extinction rates following a Poisson process, which means that the expected time to an event follows an exponential distribution (Nee 2006). In its simpler version, the birth-death model is called the Yule (or pure birth) model, in which only the speciation rate is estimated to be constant and extinction is zero. As a result, and except for the Yule and the constant birth-death models, we assume the speciation and extinction functions to be exponential. Speciation (B) and extinction (D) rates can vary through time, and both can be influenced by one or several environmental variables (e.g., temperature $T(t)$) that also varies through time. We consider the phylogeny of n species sampled from the present and allow for the possibility that some extant species are not included in the sample by assuming that each extant species was sampled with probability $f \leq 1$. Time is measured from the present to the past such that it denotes branching times in the phylogeny.

2.3.2 | Fitted Models

In total, 82 models were tested, including 2 constant-rate models, 4 time-dependent models and 76 temperature-dependent models, among which 4 models used the proxy-derived curve GATdat, and 72 models used simulation-constrained curves (Table 2, Figure 2). The two constant models, the four time-dependent models and the eight global temperature-dependent models (GATdat and GAT) were systematically fitted to all phylogenies. In addition, the four global sea surface temperature models (SST) were also fitted to the marine phylogeny of the Cetacea (for a total of 18 models) and the eight models using global continental mean annual (MAT) and winter temperature (CMT) variables were fitted for all continental phylogenies (Testudinoidea, *Pinus*, Parnassiinae, Monodorea, Arinae). 32

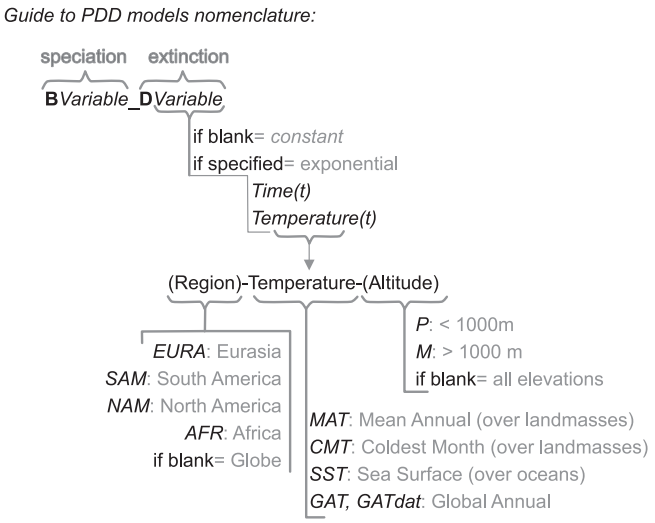

FIGURE 2 | Quick guide to the different types of PDD models used in 2.

models using the Eurasian and North American temperature curves (MAT-EURA-P, MAT-EURA-M, MAT-NAM-P, MAT-NAM-M, CMT-EURA-P, CMT-EURA-M, CMT-NAM-P, CMT-NAM-M) were fitted to the Holarctic phylogenies Parnassiinae and *Pinus*, for a total of 54 models fitted each. The Monodoreae phylogeny was also fitted with the eight models using the African temperature curves (MAT-AFR-P, CMT-AFR-P), for a total of 30 models. The Arinae phylogeny was fitted with 16 additional models based on South American temperature curves (MAT-SAM-P, MAT-SAM-M, CMT-SAM-P, CMT-SAM-M), for a total of 38 models. Finally, all regional terrestrial curves mentioned above were fitted for Testudinoidea, as they are widespread over the globe, totaling 78 models tested for this clade.

3 | Results

We first describe and interpret briefly the temperature time series obtained with the hybrid methodology depicted above. The results obtained with RPANDA are then presented in Figure 3, showing only the 20 best models for each clade, ranked by their Akaike weight (AICω). In a second step, the AICω were recalculated, comparing the best model of each category: temperature-dependent, time-dependent and constant models (Table 3). The diversification plots as generated by RPANDA for each of the best models are shown in Figures 4 and 5.

3.1 | Temperature Time Series

By construction, our hybrid global temperature time series (GAT) depicts the same trends (Figure 1a) as the proxy-derived one (GATdat). However, the temperatures serving as anchor points every 10 million years to construct GAT lead to significant differences between both time series. This is due to the very nature of the proxies used to obtain GATdat on the one side, and palaeoclimate simulations on the other. Simulated temperatures (see detailed methodology in Li et al. (2022)) were obtained through a tuning strategy aiming to match reconstructed temperatures derived mostly from the continental record. To do so, various palaeoclimate indicators over the globe (tillite, evaporites, bauxites, fossils, see Boucot et al. (2013), Scotese et al. (2021)), have been compiled to map the extent of the main Köppen climatic belts (tropical humid, warm arid, warm temperate, seasonal temperate and boreal). A mean temperature was then attributed to each belt, based on conservatism hypothesis and used to calculate the global mean annual temperature for each time step. The authors further perform some punctual adjustments to the global curve (see Scotese et al. (2021) for a full description). Thus, palaeoclimate simulations used as anchor points to produce GAT have been mostly adjusted to the continental temperature record. GATdat on the other hand, has been obtained with a radically different approach, through the conversion of $\delta^{18}O$ measured of deep-sea fossil foraminifera, first to deep-sea temperatures, then to air temperature, using the equations of Hansen et al. (2013).

These differences lead to a general offset of 1 to 3°C between GATdat and GAT. GATdat is also significantly warmer in the late Cretaceous and the early Eocene, with ~32°C at 90 Ma and ~29°C at 50 Ma for GATdat, against ~25°C for GAT during the same periods. For the present time (0 Ma), GAT (~16°C) indicates warmer temperatures than GATdat (~12°C). This latter difference is linked to the fact that the 10 million-year time span between climate simulations from Li et al. (2022) do not permit to account for the Plio-Pleistocene glacial inceptions and onsets of glacial–interglacial cycles.

While it is out of the scope of this study to debate whether one representation of global mean annual temperature is more accurate than the other, it is important to stress that it is the relative change along a time series that matters to PDD models as implemented in RPANDA, rather than the absolute temperature values (in °C). In that optic, the main changes between trends of the GATdat and GAT time series are observed in the late Cretaceous and early Eocene, with warm intervals described by GATdat, while a more equable climate is described by GAT time series. Regional time series also convey interesting perspectives: while mean annual and coldest month temperature time series tend to follow similar trends through time, the temperature evolution of plains versus mountainous regions display notable changes, especially for North American and Eurasian regions (Figure 1b,c). Although it may seem counter-intuitive at first, the temperatures in plains may be colder than the mountainous regions, especially after 40 Ma. This is due to a strong polar amplification effect on lowlands situated at high latitudes in the Holarctic region, while most of the mountains (Rockies, Appalachians, Tibetan Plateau, Iranian Plateau, Alps) are at lower latitudes.

3.2 | Performance Comparison Among Temperature-Dependent Models

3.2.1 | Performance of Models Based on Simulations-Constrained GAT Temperature Variable Compared to Models Based on the Proxy-Derived GATdat Variable

First, we evaluated the respective support received by models using the proxy-derived temperature curve GATdat, that has been the reference in previous studies involving PDD models,

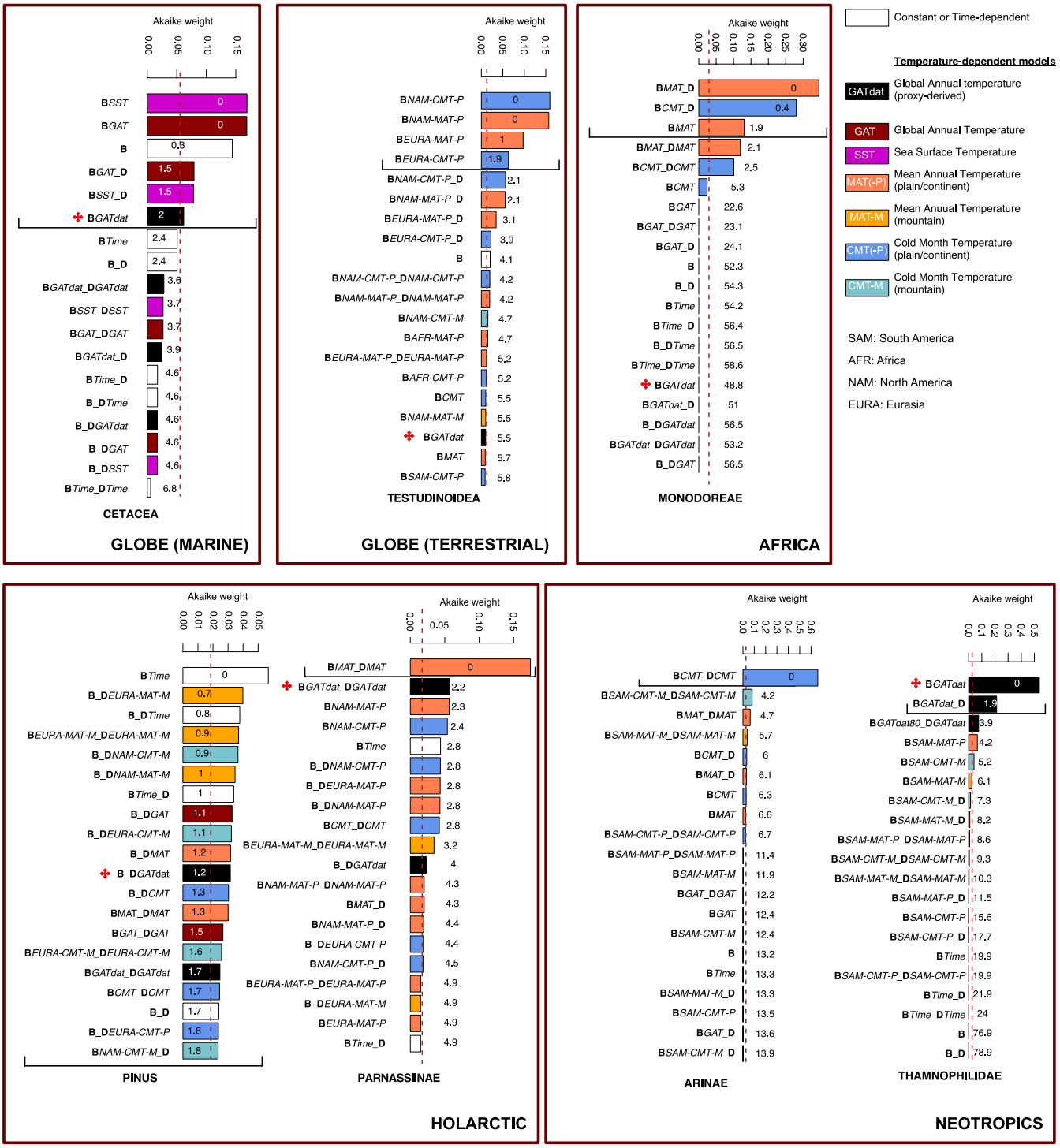

FIGURE 3 | Comparison of the Akaike weights (AICω) obtained for the 20 best models of each phylogeny. Bar colours match the colour coding of each environmental curve presented in Figure 1. Red asterisk indicates the first occurrence of a temperature-dependent model based on the variable GATdat, which is the temperature variable traditionally used in previous studies. The vertical red dotted line corresponds to the expected AICω if all models were equally likely. For each model, the ΔAICω criterion is indicated: As a convention, models with a ΔAICc < 2 are considered of equal confidence, marked by a horizontal line.

and models using the GAT curve constrained with palaeoclimate simulations (Figure 1a). For the Cetacea phylogeny (Figure 3), model B*GAT* received the highest support (AIC$\omega = 0.17$, on par with model B*SST*), while the best GATdat model (B*GATdat*) received significantly lower support (AIC$\omega = 0.06$, ninth-best model). For Apollo butterflies (Parnassiinae), the GATdat model (B*GATdat*_D*GATdat*, AIC$\omega = 0.06$, third-best model) received much higher support than any GAT models (not ranked in the top 20 models). For the *Pinus* phylogeny, model B_D*GAT* received similar support (AIC$\omega = 0.032$, eighth-best model) than the best GATdat model (B_D*GATdat*, AIC$\omega = 0.031$, eleventh-best model). In the Arinae, Monodorea and Testudinoidea

TABLE 3 | Results of the diversification analyses, showcasing the best model of each category (Constant, time-dependent, temperature-dependent, sea level-dependent).

Clade	Model	NP	logL	AICc	AICω	λ_0	α	μ_0	β
Cetacea	**B**	1	−276.789	555.626	0.40	0.106	—	—	—
	B*Time*	2	−276.786	557.716	0.14	0.107	0.001	—	—
	B*SST*	**2**	**−275.583**	**555.308**	**0.46**	**0.0017**	**0.22**	—	—
Testudinoidea	**B**	1	−605.815	1213.655	0.10	0.0619	—	—	—
	B*Time*	2	−605.751	1215.579	0.04	0.0636	0.0017	—	—
	B*NAM-CMT-P*	**2**	**−602.737**	**1209.55**	**0.85**	**0.0257**	**0.0457**	—	—
Monodoreae	**B**	1	−235.854	473.755	0	0.1773	—	—	—
	B*Time*	2	−235.804	475.75	0	0.183	0.0061	—	—
	B*MAT*_D	**3**	**−207.609**	**421.503**	**1**	**4.47e-06**	**1.1516**	**0.2429**	—
Pinus	**B_D**	2	−365.971	736.048	0.2	0.2096	—	0.1788	—
	B*Time*	**2**	**−365.103**	**734.313**	**0.47**	**0.1597**	**0.0397**	—	—
	B_D*EURA-MAT-M*	3	−364.403	735.02	0.33	0.1911	—	0.1073	0.0505
Parnassiinae	**B_D**	2	−239.56	483.267	0.02	0.2171	—	0.1245	—
	B*Time*	2	−237.398	478.943	0.20	0.2065	0.0434	—	—
	B*MAT*_D*MAT*	**4**	**−233.841**	**476.183**	**0.78**	**0.0032**	**0.4718**	**0.0016**	**0.526**
Arinae	**B**	1	−412.664	827.353	0	0.2229	—	—	—
	B*Time*	2	−411.694	827.461	0	0.2463	0.0224	—	—
	B*CMT*_D*CMT*	**4**	**−402.972**	**814.19**	**1**	**1.6007**	**0.7052**	**2.9955**	**1.2941**
Thamnophilidae	**B**	1	−657.759	1317.536	0	0.1554	—	—	—
	B*Time*	2	−628.223	1260.498	0	0.0815	0.1221	—	—
	B*GATdat*	**2**	**−618.292**	**1240.637**	**1**	**0.0018**	**0.3122**	—	—

Note: For each clade, the best-fitting model (higher AICω) is highlighted in bold. The table displays the model, the number of parameters (NP), the estimated log-likelihood (logL), the corrected Akaike information criterion (AICc), the Akaike weight of the model (AICω) and the corresponding parameter estimates (λ_0 = speciation rate at present, α = parameter controlling the dependency of speciation rate on time or environment, μ_0 = extinction rate at present and β = parameter controlling the dependency of extinction rate on time or environment).

phylogenies, neither GAT nor GATdat models received significant support (AICω close to 0). Thamnophilidae phylogeny is the only one for which GATdat models receive the highest support, with B*GATdat* model yielding an AICω = 0.53, while none of the GAT model appears in the best 20 models (Figure 3). This model translates into a burst of speciation during the Mid-Miocene Climatic Optimum, and a decrease in speciation rates towards the present (Figure 4).

3.2.2 | Performance of Models Based on the Simulation-Constrained MAT, SST, and CMT Compared to Models Based on GAT

Here, we assessed if distinguishing, at the global scale, the air temperature evolution over continental masses versus over the oceans, could yield better results for terrestrial and marine phylogenies, respectively. For Cetacea, the B*SST* model received the highest support (AICω = 0.16, Figure 3), on par with the B*GAT* model. Such a congruence is explained by the very similar trends of these two curves for the time span of the Cetacean phylogeny (last 35 Ma, Figure 1a). It is a pure birth model with a positive dependency of speciation to temperature that receives the best support (AICω = 0.46, when comparing only the three best models, Table 3). This translates into a decrease of speciation at the Eocene–Oligocene transition (33.9 Ma), followed by two increase in speciation, during the Mid-Miocene Climatic Optimum, and in the latest Miocene (Figure 3).

Regarding continental clades, two models using the mean annual temperature evolution received very high support. Parnassiinae displayed a positive correlation of both speciation and extinction to mean annual temperature (B*MAT*_D*MAT*, best model, AICω = 0.19 and AICω = 0.78 when recalculated comparing the three best models, Table 3). This is expressed through a dramatic decrease in both speciation and extinction rates during the late Eocene and at the Eocene–Oligocene Transition (40–33 Ma), followed by two minor increases in speciation and extinction during the mid-Miocene Climate Optimum (MMCO) and the latest Miocene (Figure 4). In the case of Monodoreae, the best model described a positive correlation of speciation to mean annual temperature, and a constant extinction rate (B*MAT*_D,

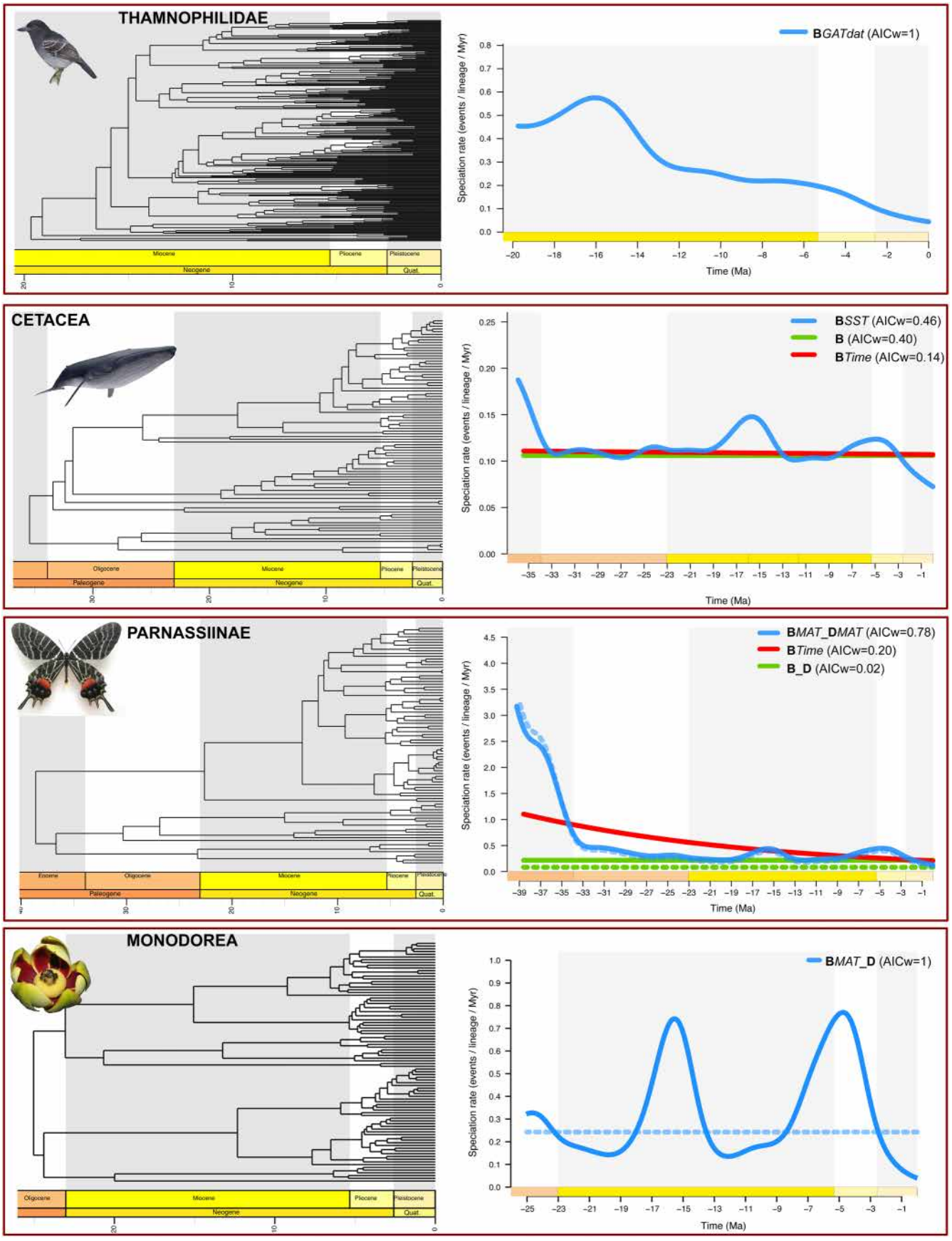

FIGURE 4 | Legend on next page.

FIGURE 4 | Potential diversification dynamics obtained with the best-fit model of each category: Constant, time-dependent and temperature-dependent. On the left panel, the dated phylogeny of each clade is presented, and on the right panel speciation (full line) and extinction (dotted line) rates are shown, together with the Akaike weights (AICω) corresponding to each model, also summed up in Table 3. Only models with non-null AICω are shown. Illustrations credits: Thamnophilidae, (Harvey et al. 2020); Parnassiinae, F.L. Condamine; Monodorea, T.L.P. Couvreur.

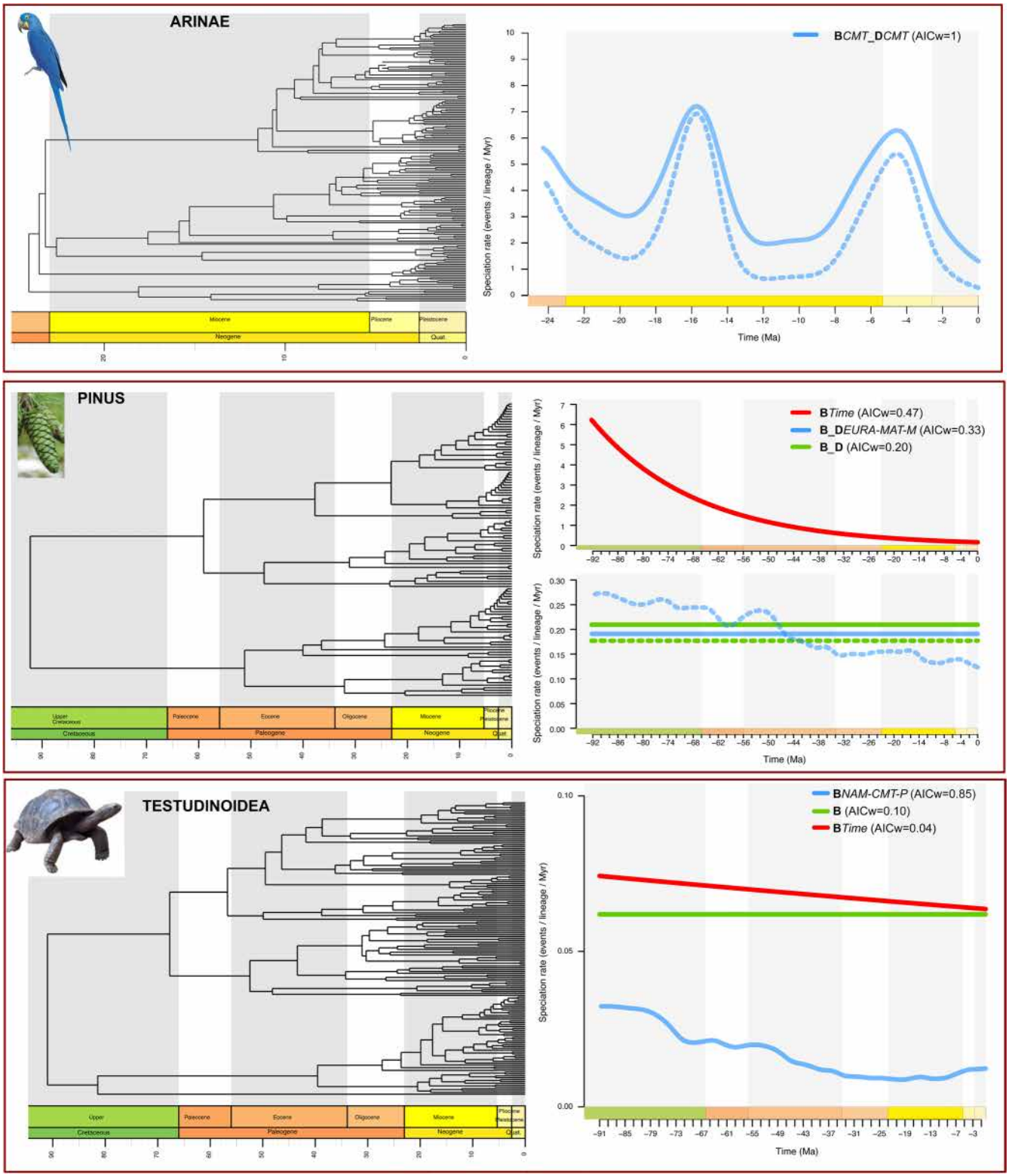

FIGURE 5 | Reader is referred to Figure 4. Illustrations credits: Arinae (Smith et al. 2023), *Pinus* (Jin et al. 2021) and Testudinoidea (Thomson et al. 2021).

best model, AIC$\omega = 0.34$, and AIC$\omega = 1$ when recalculated keeping only the three best models, Table 3). Again, two speciation peaks were inferred at the MMCO and latest Miocene, respectively (Figure 4).

Models based on the global coldest month temperature (CMT) also receive good support, for Arinae (B*CMT*_D*CMT*, best model AIC$\omega = 0.65$ and AIC$\omega = 1$ when recalculated comparing the three best models, Table 3) and for Monodoreae (B*CMT*_D, second-best, AIC$\omega = 0.28$). In the case of Arinae, both speciation and extinction rates are positively correlated to temperature, overall leading to an increased net diversification during cooler periods (Figure 5).

3.2.3 | Performance of Models Based on Simulation-Constrained Regional Mean Annual Temperature Variables

Different subsets of regional temperature variables were tested on terrestrial phylogenies, depending on their regions of occurrence and habitat affinity (as introduced in Sections 2.1 and 2.3.2). Models derived from regional time series tend to get high support for most phylogenies (Figure 3). For *Pinus*, the second-best model is based on the evolution of Eurasian mean annual temperature in mountains (B_D*EURA-MAT-M*, AIC$\omega = 0.039$), and it is also the best temperature-dependent model for this phylogeny (AIC$\omega = 0.33$ when comparing only the three best models). B_D*EURA-MAT-M* predicts a positive correlation of extinction with temperature, thus displaying higher extinction rate in the Late Cretaceous, Palaeogene and early Eocene (Figure 5).

The model B*NAM-MAT-P*, based on North American mean annual temperature evolution (in plains), is on par with the model B*NAM-CMT-P* for Testudinoidea (AIC$\omega = 0.16$) and third-best for Parnassiinae (AIC$\omega = 0.06$). We can also mention that none of the African regional models gets significant results for Monodoreae (they all receive an AIC$\omega = 0$). Similarly, most of the models using South American regional time series receive very low support for Arinae and Thamnophilidae neotropical birds.

3.2.4 | Performance of Models Based on the Simulations-Constrained Regional Winter Temperature Variables

Regional coldest month temperatures were additionally tested for terrestrial phylogenies, assuming cold may be a more critical parameter than mean annual temperature evolution for warm-adapted clades (ectotherms or tropical clades). Models based on North American coldest month temperature at low elevation (B*NAM-CMT-P*) receive high support for Testudinoidea (best model, AIC$\omega = 0.16$ and best temperature-dependent model, with an AIC$\omega = 0.85$ when considering only the three best models). This positive correlation of speciation to coldest month temperature translates into progressively decreasing speciation rates throughout most of the past 90 My, with an increase in the Pliocene (Figure 4). For *Pinus*, it is the North American winter temperature evolution in mountains (B_D*NAM-CMT-M*) that receives high support (fifth-best model, AIC$\omega = 0.037$).

3.3 | Performance of Temperature-Dependent Models Compared to Other Birth-Death Models

Temperature-dependent models overall received high support for all phylogenies. Nevertheless, pure birth or time-dependent models also receive significant support on a few occasions: B*Time* is best model for *Pinus* (AIC$\omega = 0.057$) and fifth-best for Parnassiinae, while pure birth B model is third-best model for Cetacea (AIC$\omega = 0.11$).

4 | Discussion

4.1 | Spatialised and Seasonal Palaeotemperature Curves and Their Application to Palaeoenvironment-Dependent Diversification Models

In this paper, we propose a reproducible methodology to generate user-specific spatialised and/or seasonal palaeotemperature curves. In doing so, we provide a potentially more accurate inference of regional and seasonal temperature change through the last 100 My, complementing global temperature models (Westerhold et al. 2020). For example, we can generate temperature curves for different continents and compare the climate trends through time (Figure 1). As such, our approach is highly relevant to studies in macroecology or macroevolution, where understanding past climate is central to explain observed patterns. Here, we were specifically interested in integrating these regional and/or seasonal palaeotemperature curves in palaeoenvironment-dependent diversification (PDD) models to assess how these spatialised data sets can improve, or not, our understanding of macroevolution when compared to global curves. Using seven clades displaying a variety of ecologies and distributions as case studies, we evaluated which temperature curve best explained diversification patterns. We show that, except for Thamnophilidae (Figure 3, Table 3), all phylogenetic trees were better fitted by models other than the traditionally used global atmosphere annual temperature trend derived from benthic oxygen isotopes record (GATdat) and the hybrid GAT. Below, we discuss some of our findings in relation to temperature variables. We do not pretend to explain the diversification of each clade in detail since further studies including other environmental data would be necessary.

Several clades showed high support to models based on hybrid curves that seemingly agreed with their ecology, probably better than a dependency to a global temperature trend. This is the case of the two oldest clades, *Pinus* and Testudinoidea, displaying a high correlation of diversification rates to regional temperature models of Eurasian and North American regions (Figure 3). In the case of *Pinus*, the models based on mountainous temperature evolution often received high support and were positively correlated to extinction (B_D*EURA-MAT-M*, B_D*NAM-CMT-M*, B_D*NAM-MAT-M* and B_D*EURA-CMT-M*). This may support the findings of Jin et al. (2021), who showed that mean annual temperature and topography are two key determinants of *Pinus* diversity today. Conversely, in the case of Testudinoidea, speciation rates were systematically correlated to temperature in plains (B*EURA-MAT-P*, B*NAM-CMT-P*, B*NAM-MAT-P* and B*EURA-CMT-P*). Given

the strong affinity of turtles for lowland and coastal environments (Thomson et al. 2021), this is a very promising result that demonstrates the added value of our new methodology. Given the high proportion of North American species sampled in the Testudinoidea phylogenetic tree, we can assume it may explain the high score received by NAM models in these PDD analyses, over other regions of the globe. It is worth noting that, North America, and to a lesser extent Eurasia, are regions where curves constrained with palaeoclimate simulations show the most different trends between mountainous and lowland regions (Figure 1). Therefore, a given clade is unlikely to display a strong support for both environments (while it is more common for the Neotropical clades, see Figure 3).

Additionally, models based on coldest month temperature received high support, for Testudinoidea, Monodoreae and Arinae (Figure 3). These clades being respectively ectotherm and tropical, winter temperature is expected to be an important parameter in explaining their diversification (Sakai and Larcher 2012; Donoghue 2008). For Testudinoidea, the positive correlation between speciation and North American winter temperature evolution (in plains), suggests an increase in diversification with higher winter temperatures, and slowdowns in diversification during cooling events (Figure 4), in line with previous studies (Chiarenza et al. 2023; Thomson et al. 2021). Other factors likely influenced the diversification of turtles, such as the emergence of new lands suitable for their development during periods of sea level fall (Thomson et al. 2021). Providing further research, our approach may allow understanding more precisely the relative importance of regional and seasonal temperature changes versus available space in turtles evolutionary history. In the Monodoreae case study, using the same dated phylogenetic tree, African palaeoelevation was correlated with diversification, whereas the GATdat model was not significant (Dagallier et al. 2024). Here, we show that the MAT and CMT are much better fits than GATdat, suggesting that more detailed temperature models can be preferred over global ones for tropical African clades. Finally, the high score received by the B*CMT*–D*CMT* model for Arinae also suggests a strong impact of winter climate on these parrot bird diversification dynamics. Such dependence of temperature in parrot diversification would be completely overlooked if considering only the classical global temperature trend (GATdat). A finer understanding of the potential influence of coldest month temperature on parrot diversification would nevertheless require in-depth research.

The cetacean results showed comparable support for temperature dependence (either B*SST* or B*GAT*) and for a pure birth model with constant speciation rates through time (Table 3). The high support described by the temperature-dependent models (B*SST* or B*GAT*), translating into a marked decrease in speciation at the Eocene–Oligocene transition (33 Ma), followed by two increases at the mid-Miocene Climate Optimum (17–15 Ma) and in the latest Miocene (7–8 Ma), is congruent with other studies (Marx and Uhen 2010; Condamine et al. 2013).

For Parnassiinae, the MAT variable was the only significant variable (Figure 3). However, the explanation may be less straightforward, given that Apollo butterflies are mostly present in the Palearctic and especially the Himalayan regions today (Condamine et al. 2018), and even though the curves related to seasonal (CMT) or altitude (M) showed some weight, they were not significant.

In the few case studies analysed here, we thus show that regional and seasonal palaeotemperature curves as generated here provided a more detailed understanding of the role of temperature in diversification. These approaches are prone to improvement in the future, which we discuss below.

4.2 | Challenges of Using Palaeoclimate Simulations-Derived Time Series

Our hybrid method to build environmental time series provides a framework to circumvent the impossibility of running million-year-long climate simulations with state-of-the-art Earth System Models. Here, we emphasise the points that users need to be vigilant about in using our methodology and the potential areas for improvement. First, our hybrid time series are highly influenced by (i) the palaeoclimate simulations data set, (ii) the number of available simulations over the considered time period, and (iii) the interpolation method used. A direct consequence is that the higher the number of simulations, the lesser the hybrid time series will rely on background data. Here we used an equally spaced data set (Li et al. 2022) with one simulation every 10 million years, which prevents capturing important climate transitions in between these time series (e.g., the Eocene–Oligocene transition, 33 Ma, or the Mid-Miocene Climatic Optimum, 15 Ma). As a consequence, the imprint of these events in our hybrid time series is mostly driven by the GATdat trend used as interpolation background. Therefore, to explore the specific regional expression of these climatic events more comprehensively, it would be beneficial to produce simulations that specifically target these key periods in the past. Such an approach involves the development of new palaeoclimate modelling strategies aimed at finding a compromise between computing cost and temporal precision.

Second, Model Intercomparison Projects dedicated to the geological past (e.g., MioMIP (Burls et al. 2021) or DeepMIP (Lunt et al. 2021)) have shown that there can be substantial variations between results obtained with different Earth System Models, especially at the regional scale. This is mostly attributable to differences in model spatial resolution and tuning strategy through parametrisation (Hourdin et al. 2017). As mentioned in Section 3.1, the palaeoclimate simulations from the data set used in the present study were designed to match the estimated mean global palaeotemperature reconstructed from a variety of palaeoenvironmental archives compiled in (Scotese et al. 2021) (see Li et al. (2022) for full methodology), by adjusting the pCO_2 concentration. Other palaeoclimate groups adopt a reverse strategy, which is to set a pCO_2 value in agreement with pCO_2 proxies estimates, without specifically trying to match an estimated global temperature. While both strategies have their advantages and disadvantages, it is important to acknowledge that biases from the original proxies (e.g., due to sampling bias, errors in dating or palaeolocalising the proxy, calibrations issues) may be reflected in the simulated palaeoclimate. Consequently, users of palaeoclimate model results for macroevolutionary purposes must be aware of the specific characteristics of the model, including its biases. Given the high degree of uncertainty on boundary

conditions for certain time periods, palaeoclimate simulations also depend on decision-making during their experimental design. Typically, pCO_2 estimates have long been quite uncertain in the geological past (Foster et al. 2017, The Cenozoic CO_2 Proxy Integration Project (CENC02PIP) Consortium 2023, Rae et al. 2021) and palaeogeographic reconstructions may entail uncertainties, due to the lack of available data or conflicting results with different methods (Buffan et al. 2023; Poblete et al. 2021; Tardif et al. 2023; Botsyun et al. 2019; Su et al. 2019). While these uncertainties have been reduced considerably during the past decades, palaeogeographic reconstructions are bound to further improve with time and access to new data, which may lead to revision of palaeoelevation, mountains extant, drainage patterns and land-sea distribution. While the impact of a particular geographic feature will likely be smoothed if working with a temperature time series at the global or continental scale, it may lead to significant changes when working on clades at the regional to local scale.

Future studies would also benefit from comparing thoroughly the time series generated with our initial approach with those obtained with recent emulators and data assimilation strategies. Although, to our knowledge, emulators have been applied to notably shorter time intervals of a few My so far (e.g., the Pliocene and the Eocene–Oligocene Transition, see Van Breedam et al. (2022), Lord et al. (2017)) using them with high-resolution Earth System Models over the entire Cenozoic could open new avenues to include environmental variables in diversification models. Likewise, our reconstructions could be compared to global temperatures reconstructed through the use of palaeoclimate data assimilation methods that combine the use of a high number of palaeoclimate simulations with various palaeotemperature reconstructions (see (Judd et al. 2024), published very recently).

4.3 | Perspectives

Our original endeavour to include climate model-derived information into the PDD framework can be enhanced in several ways and open doors to new studies. First, besides temperature, rainfall or available continental surface have also likely been key drivers of diversification (Fine and Ree 2006; Zaffos et al. 2017; Neves et al. 2021; Ringelberg et al. 2023; Husson and Sepulchre 2021). Including rainfall into new exploratory environmental time series could be fruitful, but is still very challenging. It requires overcoming important limitations in the way rainfall can be interpolated, since there is no time-continuous proxy for palaeoprecipitation variations through time. In addition, although improvements have been made in the latest generations, Earth System Models are known to have limitations in their ability to simulate rainfall (Stevens and Bony 2013), calling for a careful comparison between palaeoproxies and model outputs before using them within a PDD framework. Including other abiotic forcings (like palaeogeography or pCO_2) will allow to explicitly test which variable, or which combination of variables, better explains diversification (e.g., Condamine et al. 2015, 2018; Boschman and Condamine 2022).

Our diversification analyses with the PDD models make the assumption of a single rate depending on the environment Condamine et al. (2013), which can be an oversimplification of the diversification history of the group. For example, Morlon et al. (2011) showed that it is necessary to account for rate heterogeneity, with different groups having different diversification dynamics, in order to reconcile the observed discrepancy between phylogenetic data and the fossil record. It is also possible that subclades responded differently to environmental changes (e.g., Condamine et al. 2012; Quintero et al. 2023). Accordingly, allowing PDD models to account for climate heterogeneity in diversification rates, that is, multiple regional climate curves applied to different clades rather than a single curve for the whole group, would be a significant step forward in macroevolutionary studies. While the estimation of clade-specific diversification rates has recently been automated and improved in RPANDA (Mazet et al. 2023), it has yet to be adapted to a palaeoenvironmental context.

Finally, our methodology may be of interest to produce the abiotic fields needed to force the emerging generation of population-based, spatially explicit, mechanistic eco-evolutionary models (e.g., Rangel et al. (2018), Hagen et al. (2021), see Hagen (2023) for a review). Nevertheless, these new models require the use of environmental records (aridity index, temperature and elevation) with a high spatial resolution, which represent an additional challenge to be tackled.

5 | Conclusions

The present study demonstrated the strong potential of generating spatialised and seasonal proxy-derived temperature trends constrained with palaeoclimate simulations, and how these can then be integrated into environment-dependent diversification models. As such, we can test more detailed diversification hypotheses like the influence of global to regional and/or seasonal temperature trends on the speciation and extinction dynamics of a given clade. This new methodology, when used in combination with biogeographic analyses, the integration of fossil information and other macroevolutionary data, may significantly advance our understanding of how abiotic factors impact biodiversity patterns.

Author Contributions

D.T., F.L.C., T.L.P.C. and P.S. jointly designed the methodology. D.T. led the methodological framework, extracted the climatic data, designed the time interpolation of palaeoclimate variables, conducted all analyses, and drafted the initial version of the article. F.L.C. provided expertise in the use and interpretation of RPANDA outputs. F.L.C., T.L.P.C. and S.J.R.S. provided expertise in the selection of phylogenetic trees and interpretation of the results. P.S. provided the original idea to include information from palaeoclimate numerical simulations in the PDD model and expertise in the comparison of palaeoclimate modelling-derived time series and proxy-derived temperature time series. All authors contributed to the writing and discussion of the results.

Acknowledgements

We thank Christophe Bessin for his expert counsel in the use of geostatistical kriging methods. Figures were done using R and NOAA pyferret within Jupyter notebooks, thanks to the ferretmagic add-on developed at LSCE by Patrick Brockmann. Ferret is a product of NOAA's

Pacific Marine Environmental Laboratory. Information is available at http://ferret.pmel.noaa.gov/Ferret (last access: 1 January 2022; NOAA's Pacific Marine Environmental Laboratory, 2020), distributed under the Open Source Definition. The Jupyter notebook is an open-source web application.

Conflicts of Interest

The authors declare no conflicts of interest.

Data Availability Statement

Files needed (scripts and data) are present on the following Zenodo repository: https://doi.org/10.5281/zenodo.14252952.

References

Allio, R., B. Nabholz, S. Wanke, et al. 2021. "Genome-Wide Macroevolutionary Signatures of Key Innovations in Butterflies Colonizing New Host Plants." *Nature Communications* 12, no. 1: 354. https://doi.org/10.1038/s41467-020-20507-3.

Boschman, L., and F. Condamine. 2022. "Mountain Radiations Are Not Only Rapid and Recent: Ancient Diversification of South American Frog and Lizard Families Related to Paleogene Andean Orogeny and Cenozoic Climate Variations." *Global and Planetary Change* 208: 103704. https://doi.org/10.1016/j.gloplacha.2021.103704.

Botsyun, S., P. Sepulchre, Y. Donnadieu, C. Risi, A. Licht, and J. K. Caves Rugenstein. 2019. "Revised Paleoaltimetry Data Show Low Tibetan Plateau Elevation During the Eocene." *Science* 363, no. 6430: eaaq1436. https://doi.org/10.1126/science.aaq1436.

Boucot, A. J., C. Xu, C. R. Scotese, and R. J. Morley. 2013. *Phanerozoic Paleoclimate: An Atlas of Lithologic Indicators of Climate*. SEPM (Society for Sedimentary Geology). https://pubs.geoscienceworld.org/books/book/1966/.

Buffan, L., L. Jones, M. Domeier, C. Scotese, S. Zahirovic, and S. Varela. 2023. "Mind the Uncertainty: Global Plate Model Choice Impacts Deep-Time Palaeobiological Studies." *Methods in Ecology and Evolution* 14, no. 12: 3007–3019. https://doi.org/10.1111/2041-210X.14204.

Burls, N. J., C. D. Bradshaw, A. M. D. Boer, et al. 2021. "Simulating Miocene Warmth: Insights From an Opportunistic Multi-Model Ensemble (MioMIP1)." *Paleoceanography and Paleoclimatology* 36, no. 5: e2020PA004054. https://doi.org/10.1029/2020PA004054.

Chatrou, L. W., M. D. Pirie, R. Erkens, et al. 2012. "A New Subfamilial and Tribal Classification of the Pantropical Flowering Plant Family Annonaceae Informed by Molecular Phylogenetics: ANNONACEAE PHYLOGENETICS AND CLASSIFICATION." *Botanical Journal of the Linnean Society* 169, no. 1: 5–40. https://doi.org/10.1111/j.1095-8339.2012.01235.x.

Chiarenza, A., A. Waterson, D. Schmidt, et al. 2023. "100 Million Years of Turtle Paleoniche Dynamics Enable the Prediction of Latitudinal Range Shifts in a Warming World." *Current Biology: CB* 33, no. 1: 109–121.e3. https://doi.org/10.1016/j.cub.2022.11.056.

Condamine, F. L., J. Rolland, S. Höhna, F. A. H. Sperling, and I. Sanmartín. 2018. "Testing the Role of the Red Queen and Court Jester as Drivers of the Macroevolution of Apollo Butterflies." *Systematic Biology* 67, no. 6: 940–964. https://doi.org/10.1093/sysbio/syy009.

Condamine, F. L., J. Rolland, and H. Morlon. 2013. "Macroevolutionary Perspectives to Environmental Change." *Ecology Letters* 16, no. s1: 72–85. https://doi.org/10.1111/ele.12062.

Condamine, F. L., J. Rolland, and H. Morlon. 2019. "Assessing the Causes of Diversification Slowdowns: Temperature-Dependent and Diversity-Dependent Models Receive Equivalent Support." *Ecology Letters* 22, no. 11: 1900–1912. https://doi.org/10.1111/ele.13382.

Condamine, F. L., F. A. H. Sperling, N. Wahlberg, J. Y. Rasplus, and G. J. Kergoat. 2012. "What Causes Latitudinal Gradients in Species Diversity? Evolutionary Processes and Ecological Constraints on Swallowtail Biodiversity." *Ecology Letters* 15, no. 3: 267–277. https://doi.org/10.1111/j.1461-0248.2011.01737.x.

Condamine, F. L., E. F. A. Toussaint, A. L. Clamens, G. Genson, F. A. H. Sperling, and G. J. Kergoat. 2015. "Deciphering the Evolution of Birdwing Butterflies 150 Years After Alfred Russel Wallace." *Scientific Reports* 5, no. 1: 11860. https://doi.org/10.1038/srep11860.

Couvreur, T. L. P. 2009. *Monograph of the Syncarpous African Genera Isolona and Monodora (Annonaceae)*. American Society of Plant Taxonomists. OCLC: 424500805.

Dagallier, L. P. M. J., F. L. Condamine, and T. L. P. Couvreur. 2024. "Sequential Diversification With Miocene Extinction and Pliocene Speciation Linked to Mountain Uplift Explains the Diversity of the African Rain Forest Clade Monodoreae (Annonaceae)." *Annals of Botany* 133, no. 5-6: mcad130. https://doi.org/10.1093/aob/mcad130.

Dagallier, L. P. M. J., F. M. Mbago, M. Couderc, et al. 2023. "Phylogenomic Inference of the African Tribe Monodoreae (Annonaceae) and Taxonomic Revision of Dennettia, Uvariodendron and Uvariopsis." *PhytoKeys* 233: 1–200. https://doi.org/10.3897/phytokeys.233.103096.

Dapporto, L. 2009. "Speciation in Mediterranean Refugia and Post-Glacial Expansion of Zerynthia Polyxena (Lepidoptera, Papilionidae)." *Journal of Zoological Systematics and Evolutionary Research* 48, no. 3: 229–237. https://doi.org/10.1111/j.1439-0469.2009.00550.x.

Davis, K. E., J. Hill, T. I. Astrop, and M. A. Wills. 2016. "Global Cooling as a Driver of Diversification in a Major Marine Clade." *Nature Communications* 7, no. 1: 13003. https://doi.org/10.1038/ncomms13003.

Delsuc, F., S. F. Vizcano, and E. J. Douzery. 2004. "Influence of Tertiary Paleoenvironmental Changes on the Diversification of South American Mammals: A Relaxed Molecular Clock Study Within Xenarthrans." *BMC Evolutionary Biology* 4: 11. https://doi.org/10.1186/1471-2148-4-11.

Donoghue, M. J. 2008. "A Phylogenetic Perspective on the Distribution of Plant Diversity." *Proceedings of the National Academy of Sciences* 105, no. Supplement 1: 11549–11555. https://doi.org/10.1073/pnas.0801962105.

Ezard, T., T. Quental, and M. Benton. 2016. "The Challenges to Inferring the Regulators of Biodiversity in Deep Time." *Philosophical Transactions of the Royal Society of London. Series B, Biological Sciences* 371, no. 1691: 20150216. https://doi.org/10.1098/rstb.2015.0216.

Favre, A., M. Päckert, S. U. Pauls, et al. 2015. "The Role of the Uplift of the Qinghai-Tibetan Plateau for the Evolution of Tibetan Biotas." *Biological Reviews* 90, no. 1: 236–253. https://doi.org/10.1111/brv.12107.

Fine, P., and R. Ree. 2006. "Evidence for a Time-Integrated Species-Area Effect on the Latitudinal Gradient in Tree Diversity." *American Naturalist* 168, no. 6: 796–804. https://doi.org/10.1086/508635.

Foster, G. L., D. L. Royer, and D. J. Lunt. 2017. "Future Climate Forcing Potentially Without Precedent in the Last 420 Million Years." *Nature Communications* 8, no. 1: 14845. https://doi.org/10.1038/ncomms14845.

Hagen, O. 2023. "Coupling Eco-Evolutionary Mechanisms With Deep-Time Environmental Dynamics to Understand Biodiversity Patterns." *Ecography* 2023, no. 4: e06132. https://doi.org/10.1111/ecog.06132.

Hagen, O., B. Flück, F. Fopp, et al. 2021. "gen3sis: A General Engine for Eco-Evolutionary Simulations of the Processes That Shape Earth's Biodiversity." *PLoS Biology* 19, no. 7: e3001340. https://doi.org/10.1371/journal.pbio.3001340.

Hansen, J., M. Sato, G. Russell, and P. Kharecha. 2013. "Climate Sensitivity, Sea Level and Atmospheric Carbon Dioxide." *Philosophical Transactions. Series A, Mathematical, Physical, and Engineering Sciences* 371, no. 2001: 20120294. https://doi.org/10.1098/rsta.2012.0294.

Harvey, M. G., G. A. Bravo, S. Claramunt, et al. 2020. "The Evolution of a Tropical Biodiversity Hotspot." *Science* 370, no. 6522: 1343–1348. https://doi.org/10.1126/science.aaz6970.

Hengl, T., G. Heuvelink, and D. Rossiter. 2007. "About Regression-Kriging: From Equations to Case Studies." *Computers & Geosciences* 33, no. 10: 1301–1315. https://doi.org/10.1016/j.cageo.2007.05.001.

Hoorn, C., F. P. Wesselingh, H. ter Steege, et al. 2010. "Amazonia Through Time: Andean Uplift, Climate Change, Landscape Evolution, and Biodiversity." *Science* 330, no. 6006: 927–931. https://doi.org/10.1126/science.1194585.

Hourdin, F., T. Mauritsen, A. Gettelman, et al. 2017. "The Art and Science of Climate Model Tuning." *Bulletin of the American Meteorological Society* 98, no. 3: 589–602. https://doi.org/10.1175/BAMS-D-15-00135.1.

Husson, L., and P. Sepulchre. 2021. "Geophysical Biogeography." In *Biogeography: An Integrative Approach of the Evolution of Living*, 81–113. Wiley.

Jaramillo, C., M. J. Rueda, and G. Mora. 2006. "Cenozoic Plant Diversity in the Neotropics." *Science* 311, no. 5769: 1893–1896. https://doi.org/10.1126/science.1121380.

Jin, W. T., D. S. Gernandt, C. Wehenkel, X. M. Xia, X. X. Wei, and X. Q. Wang. 2021. "Phylogenomic and Ecological Analyses Reveal the Spatiotemporal Evolution of Global Pines." *Proceedings of the National Academy of Sciences* 118, no. 20: e2022302118. https://doi.org/10.1073/pnas.2022302118.

Judd, E. J., J. E. Tierney, D. J. Lunt, et al. 2024. "A 485-Million-Year History of Earth's Surface Temperature." *Science* 385, no. 6715: eadk3705. https://doi.org/10.1126/science.adk3705.

Lagomarsino, L. P., F. L. Condamine, A. Antonelli, A. Mulch, and C. C. Davis. 2016. "The Abiotic and Biotic Drivers of Rapid Diversification in Andean Bellflowers (Campanulaceae)." *New Phytologist* 210, no. 4: 1430–1442. https://doi.org/10.1111/nph.13920.

Leslie, A. B., J. Beaulieu, G. Holman, et al. 2018. "An Overview of Extant Conifer Evolution From the Perspective of the Fossil Record." *American Journal of Botany* 105, no. 9: 1531–1544. https://doi.org/10.1002/ajb2.1143.

Lewitus, E., L. Bittner, S. Malviya, C. Bowler, and H. Morlon. 2018. "Clade-Specific Diversification Dynamics of Marine Diatoms Since the Jurassic." *Nature Ecology & Evolution* 2, no. 11: 1715–1723. https://doi.org/10.1038/s41559-018-0691-3.

Lewitus, E., and H. Morlon. 2018. "Detecting Environment-Dependent Diversification From Phylogenies: A Simulation Study and Some Empirical Illustrations." *Systematic Biology* 67, no. 4: 576–593. https://doi.org/10.1093/sysbio/syx095.

Li, X., Y. Hu, J. Guo, et al. 2022. "A High-Resolution Climate Simulation Dataset for the Past 540 Million Years." *Scientific Data* 9, no. 1: 371. https://doi.org/10.1038/s41597-022-01490-4.

Lord, N. S., M. Crucifix, D. J. Lunt, et al. 2017. "Emulation of Long-Term Changes in Global Climate: Application to the Late Pliocene and Future." *Climate of the Past* 13, no. 11: 1539–1571. https://doi.org/10.5194/cp-13-1539-2017.

Lunt, D. J., F. Bragg, W. L. Chan, et al. 2021. "DeepMIP: Model Intercomparison of Early Eocene Climatic Optimum (EECO) Large-Scale Climate Features and Comparison With Proxy Data." *Climate of the Past* 17, no. 1: 203–227. https://doi.org/10.5194/cp-17-203-2021.

Marx, F., and M. Uhen. 2010. "Climate, Critters, and Cetaceans: Cenozoic Drivers of the Evolution of Modern Whales." *Science (New York, N.Y.)* 327, no. 5968: 993–996. https://doi.org/10.1126/science.1185581.

Mazet, N., H. Morlon, P. H. Fabre, and F. L. Condamine. 2023. "Estimating Clade-Specific Diversification Rates and Palaeodiversity Dynamics From Reconstructed Phylogenies." *Methods in Ecology and Evolution* 14, no. 10: 2575–2591. https://doi.org/10.1111/2041-210X.14195.

Morlon, H., E. Lewitus, F. L. Condamine, M. Manceau, J. Clavel, and J. Drury. 2016. "RPANDA: An R Package for Macroevolutionary Analyses on Phylogenetic Trees." *Methods in Ecology and Evolution* 7, no. 5: 589–597. https://doi.org/10.1111/2041-210X.12526.

Morlon, H., T. L. Parsons, and J. B. Plotkin. 2011. "Reconciling Molecular Phylogenies With the Fossil Record." *Proceedings of the National Academy of Sciences* 108, no. 39: 16327–16332. https://doi.org/10.1073/pnas.1102543108.

Mosbrugger, V., T. Utescher, and D. L. Dilcher. 2005. "Cenozoic Continental Climatic Evolution of Central Europe." *Proceedings of the National Academy of Sciences* 102, no. 42: 14964–14969. https://doi.org/10.1073/pnas.0505267102.

Nee, S. 2006. "Birth-Death Models in Macroevolution." *Annual Review of Ecology, Evolution, and Systematics* 37, no. 1: 1–17. https://doi.org/10.1146/annurev.ecolsys.37.091305.110035.

Nee, S., R. M. May, and P. H. Harvey. 1994. "The Reconstructed Evolutionary Process." *Royal Society* 344, no. 1309: 305–311. https://doi.org/10.1098/rstb.1994.0068.

Neubauer, T., M. Harzhauser, J. Hartman, et al. 2022. "Short-Term Paleogeographic Reorganizations and Climate Events Shaped Diversification of North American Freshwater Gastropods Over Deep Time." *Scientific Reports* 12, no. 1: 15572. https://doi.org/10.1038/s41598-022-19759-4.

Neves, D., A. Kerkhoff, S. Echeverria-Londono, et al. 2021. "The Adaptive Challenge of Extreme Conditions Shapes Evolutionary Diversity of Plant Assemblages at Continental Scales." *Proceedings of the National Academy of Sciences of the United States of America* 118, no. 37: e2021132118. https://doi.org/10.1073/pnas.2021132118.

Nobis, M., C. Traiser, and A. Roth-Nebelsick. 2012. "Latitudinal Variation in Morphological Traits of the Genus Pinus and Its Relation to Environmental and Phylogenetic Signals." *Plant Ecology and Diversity* 5, no. 1: 1–11. https://doi.org/10.1080/17550874.2012.687501.

Pebesma, E. J. 2004. "Multivariable Geostatistics in S: The Gstat Package." *Computers & Geosciences* 30, no. 7: 683–691. https://doi.org/10.1016/j.cageo.2004.03.012.

Poblete, F., G. Dupont-Nivet, A. Licht, et al. 2021. "Towards Interactive Global Paleogeographic Maps, New Reconstructions at 60, 40 and 20 ma." *Earth-Science Reviews* 214: 103508. https://doi.org/10.1016/j.earscirev.2021.103508.

Quintero, I., M. J. Landis, W. Jetz, and H. Morlon. 2023. "The Build-Up of the Present-Day Tropical Diversity of Tetrapods." *Proceedings of the National Academy of Sciences* 120, no. 20: e2220672120. https://doi.org/10.1073/pnas.2220672120.

Rae, J. W., Y. G. Zhang, X. Liu, G. L. Foster, H. M. Stoll, and R. D. Whiteford. 2021. "Atmospheric CO_2 Over the Past 66 Million Years From Marine Archives." *Annual Review of Earth and Planetary Sciences* 49, no. 1: 609–641. https://doi.org/10.1146/annurev-earth-082420-063026.

Rangel, T. F., N. R. Edwards, P. B. Holden, et al. 2018. "Modeling the Ecology and Evolution of Biodiversity: Biogeographical Cradles, Museums, and Graves." *Science* 361, no. 6399: eaar5452. https://doi.org/10.1126/science.aar5452.

Ringelberg, J., E. Koenen, B. Sauter, et al. 2023. "Precipitation Is the Main Axis of Tropical Plant Phylogenetic Turnover Across Space and Time." *Science Advances* 9, no. 7: eade4954. https://doi.org/10.1126/sciadv.ade4954.

Sakai, A., and W. Larcher. 2012. *Frost Survival of Plants: Responses and Adaptation to Freezing Stress*. Vol. 62. Springer Science & Business Media.

Scotese, C. R., H. Song, B. J. Mills, and D. G. van der Meer. 2021. "Phanerozoic Paleotemperatures: The Earth's Changing Climate

During the Last 540 Million Years." *Earth-Science Reviews* 215: 103503. https://doi.org/10.1016/j.earscirev.2021.103503.

Scotese, C. R., and N. M. Wright. 2018. "PALEOMAP Paleodigital Elevation Models (PaleoDEMS) for the Phanerozoic." https://zenodo.org/record/5348492.

Smith, B. T., J. Merwin, K. L. Provost, et al. 2023. "Phylogenomic Analysis of the Parrots of the World Distinguishes Artifactual From Biological Sources of Gene Tree Discordance." *Systematic Biology* 72, no. 1: 228–241. https://doi.org/10.1093/sysbio/syac055.

Steeman, M. E., M. B. Hebsgaard, R. E. Fordyce, et al. 2009. "Radiation of Extant Cetaceans Driven by Restructuring of the Oceans." *Systematic Biology* 58, no. 6: 573–585. https://doi.org/10.1093/sysbio/syp060.

Stevens, B., and S. Bony. 2013. "What Are Climate Models Missing?" *Science* 340, no. 6136: 1053–1054. https://doi.org/10.1126/science.1237554.

Su, T., A. Farnsworth, R. Spicer, and J. Huang. 2019. "No High Tibetan Plateau Until the Neogene." *Science Advances* 5, no. 3: eaav2189. https://doi.org/10.1126/sciadv.aav2189.

Tardif, D., A. C. Sarr, F. Fluteau, et al. 2023. "The Role of Paleogeography in Asian Monsoon Evolution: A Review and New Insights from Climate Modelling." *Earth-Science Reviews* 243: 104464. https://doi.org/10.1016/j.earscirev.2023.104464.

The Cenozoic CO_2 Proxy Integration Project (CENCO2PIP) Consortium. 2023. "Toward a Cenozoic History of Atmospheric CO_2." *Science* 382, no. 6675: eadi5177. https://doi.org/10.1126/science.adi5177.

Thomson, R. C., P. Q. Spinks, and H. B. Shaffer. 2021. "A Global Phylogeny of Turtles Reveals a Burst of Climate-Associated Diversification on Continental Margins." *Proceedings of the National Academy of Sciences of the United States of America* 118, no. 7: e2012215118. https://doi.org/10.1073/pnas.2012215118.

Todisco, V., P. Gratton, D. Cesaroni, and V. Sbordoni. 2010. "Phylogeography of *Parnassius apollo*: Hints on Taxonomy and Conservation of a Vulnerable Glacial Butterfly Invader." *Biological Journal of the Linnean Society* 101, no. 1: 169–183. https://doi.org/10.1111/j.1095-8312.2010.01476.x.

Todisco, V., P. Gratton, C. Wheat, E. Zakharov, V. Sbordoni, and F. Sperling. 2012. "Mitochondrial Phylogeography of the Holarctic *Parnassius phoebus* Complex Supports a Recent Refugial Model for Alpine Butterflies." *Journal of Biogeography* 39, no. 6: 1058–1072. https://doi.org/10.1111/j.1365-2699.2011.02675.x.

Valdes, P. J., C. R. Scotese, and D. J. Lunt. 2021. "Deep Ocean Temperatures Through Time." *Climate of the Past* 17, no. 4: 1483–1506. https://doi.org/10.5194/cp-17-1483-2021.

Van Breedam, J., P. Huybrechts, and M. Crucifix. 2021. "A Gaussian Process Emulator for Simulating Ice Sheet–Climate Interactions on a Multi-Million-Year Timescale: CLISEMv1.0." *Geoscientific Model Development* 14, no. 10: 6373–6401. https://doi.org/10.5194/gmd-14-6373-2021.

Van Breedam, J., P. Huybrechts, and M. Crucifix. 2022. "Modelling Evidence for Late Eocene Antarctic Glaciations." *Earth and Planetary Science Letters* 586: 117532. https://doi.org/10.1016/j.epsl.2022.117532.

Veizer, J., and A. Prokoph. 2015. "Temperatures and Oxygen Isotopic Composition of Phanerozoic Oceans." *Earth-Science Reviews* 146: 92–104. https://doi.org/10.1016/j.earscirev.2015.03.008.

Weppe, R., F. Condamine, G. Guinot, J. Maugoust, and M. Orliac. 2023. "Drivers of the Artiodactyl Turnover in Insular Western Europe at the Eocene–Oligocene Transition." *Proceedings of the National Academy of Sciences of the United States of America* 120, no. 52: 1–11. https://doi.org/10.1073/pnas.2309945120.

Westerhold, T., N. Marwan, A. J. Drury, et al. 2020. "An Astronomically Dated Record of Earth's Climate and Its Predictability Over the Last 66 Million Years." *Science* 369, no. 6509: 1383–1387. https://doi.org/10.1126/science.aba6853.

Zachos, J., M. Pagani, L. Sloan, E. Thomas, and K. Billups. 2001. "Trends, Rhythms, and Aberrations in Global Climate 65 ma to Present." *Science* 292, no. 5517: 686. https://doi.org/10.1126/science.1059412.

Zaffos, A., S. Finnegan, and S. E. Peters. 2017. "Plate Tectonic Regulation of Global Marine Animal Diversity." *Proceedings of the National Academy of Sciences of the United States of America* 114, no. 22: 5653–5658. https://doi.org/10.1073/pnas.1702297114.

Zinetti, F., L. Dapporto, A. Vovlas, et al. 2013. "When the Rule Becomes the Exception. No Evidence of Gene Flow Between Two Zerynthia Cryptic Butterflies Suggests the Emergence of a New Model Group." *PLoS One* 8: e65746. https://doi.org/10.1371/journal.pone.0065746.

Supporting Information

Additional supporting information can be found online in the Supporting Information section.